

Pulse testing in Geothermal Energy: Demonstration of a new monitoring tool.

*Original*

Pulse testing in Geothermal Energy: Demonstration of a new monitoring tool / Fokker, P. A.; Viberti, D.; Salina Borello, E.; Verga, F.; van Wees, J. D.; de Wijkerslooth, C.; Bekius, H.; Konijn, A.; Bos, W.; Koenen, M.; van Pul-Verboom, V.. - (2022). (Intervento presentato al convegno European Geothermal Congress 2022 tenutosi a Berlin nel 17-21 October 2022).

*Availability:*

This version is available at: 11583/2978444 since: 2023-05-11T08:13:53Z

*Publisher:*

European Geothermal Energy Council

*Published*

DOI:

*Terms of use:*

This article is made available under terms and conditions as specified in the corresponding bibliographic description in the repository

*Publisher copyright*

(Article begins on next page)

## Pulse Testing in Geothermal Energy: Demonstration of a New Monitoring Tool

Peter A. Fokker<sup>1,2</sup>, Dario Viberti<sup>2</sup>, Eloisa Salina Borello<sup>2</sup>, Francesca Verga<sup>2</sup>, Jan-Diederik van Wees<sup>1,3</sup>, Charlotte de Wijkerslooth<sup>4</sup>, Hedwich Bekius<sup>4</sup>, Arjan Konijn<sup>5</sup>, Wim Bos<sup>5</sup>, Mariëlle Koenen<sup>1</sup>, Viola van Pul-Verboom<sup>1</sup>

<sup>1</sup> TNO Energy Transition, Utrecht, The Netherlands

<sup>2</sup> Politecnico di Torino, Turin, Italy

<sup>3</sup> Utrecht University, Utrecht, The Netherlands

<sup>4</sup> HVC Groep, The Netherlands

<sup>5</sup> ECW Energy, Middenmeer, The Netherlands

peter.fokker@tno.nl

**Keywords:** Monitoring, Pulse testing, Thermal front.

### ABSTRACT

Harmonic pulse testing has been employed to identify the thermal front in a geothermal system and in a heat storage system. For the geothermal system we could identify the hydraulic reservoir properties around the well. Operational constraints in combination with the distance to the thermal front precluded its identification using this test. For the heat storage, however, we did identify the heat front. After a season of injection of hot water, the heat front had propagated into the reservoir to 100 m from the well. This was in line with the value calculated from a volume and heat balance on the basis of the amount of hot water injected, the height of the reservoir and the respective heat capacities.

### 1. INTRODUCTION

Pulse testing, both for geothermal doublets and for high-temperature aquifer storage, has recently been demonstrated in a theoretical model study to have potential for the identification of temperature and thermal radius of cooled or heated zones (Fokker et al, 2021). This potential is related to the large contrast in mobility between water of different temperature, and the development of zones of altered temperature around an injector well – be it the cold injector in a geothermal doublet or the hot injector in a storage system.

This paper shows the results of pulse testing in these two applications in actual systems. The first application was in a geothermal system in two injection wells, one of which was new while the other had been in operation already for two years. The second application was in a shallow high-temperature heat storage system, where a baseline test was run prior to storing the heat and a monitoring test after 6 months of injection.

After a brief description of the two systems and the test setup we will present the test results. We close this contribution with a summary of the findings obtained and their meaning, and the possibilities, impossibilities and challenges of pulse testing for thermal front monitoring.

### 2. SYSTEM DESCRIPTION AND OPERATIONAL SETUP

#### 2.1 The Tests in the Geothermal System

The geothermal system that we deployed exists of four wells: two injection wells and two production wells. The distance between the wells is typically 1 – 2 km, so interference at the timescale of the pulse tests (up to 5 hours total duration) is not expected. The permeability of the reservoir is high: 500 – 2000 mD. The thickness of the reservoir ranges from 26 m to 39 m; the depth is 2300 m with an initial downhole temperature of 85 °C. Injection and production is scheduled to be in balance – with variations allowed insofar the volume mismatch can be collected in a number of tanks at the surface.

The first doublet, with injector I1 and producer P1, has been in operation since June 2019. The second doublet, with injector I2 and producer P2, has been recently drilled and they have been put onstream in July 2021.

The intention of the test in the geothermal system was to make a baseline pulse test on injector I2 after completion of its drilling and initial testing, and come back after a considerable amount of time to validate the concept of thermal front monitoring. As it has been outlined in Fokker et al (2021), a baseline is important for identifying the pulse testing peculiarities in that system, building trust in the technology and obtain a more robust estimate of the thermal front: a comparison of the two tests will enable the identification of the cooling solely, while excluding effects as reservoir heterogeneities and reservoir boundaries.

Besides the requirement of relatively small discrepancies between production and injection in the complete system, there was the requirement of delivering an amount of heat that had been agreed with the customers. Therefore the injection test in I2 was alternated with injection in I1. This provided two simultaneous tests in the two wells.

The design of the pulse test was made on the basis of data already available: permeability, skin, reservoir geometry. The constraint of the first test was that it should fit in a normal working day. This was necessary both for the need of operational supervision and for ensuring that the background rate would not be required to change. Therefore a scheme of 5 pulses of 2x30 minutes was employed, with rates in I1 at

increased levels when rates in I2 were decreased, and vice versa. Care was taken to precisely switch, so the pulses were all as equal as possible. Pressures were recorded at the wellhead.

### 2.2 The High-Temperature Heat Store System

The high-temperature storage consists of two wells at about 370 m depth into a high-permeability sand layer. The intention is to use the storage to improve the efficiency of a connected geothermal system. By storing excess heat in the summer and producing it back in the winter a larger maximum power can be obtained.

The injection well is a large-diameter well in which four tubings reach to depths between 30 and 42 m. One of these is used for injecting the water, the other three are employed as pressure gauges from which the pressure perturbations near the surface are removed. Temperature was measured at the wellbore and just below the pump at a depth of 135 m.

The storage system has been drilled recently and has come into operation in May 2021. A first baseline pulse test has been performed in May 2021, when no heat storage had yet taken place. A second pulse test has been performed in January 2022, when the storage for the summer season had stopped but production had not yet started. This provided us with the opportunity to compare the two test results and hopefully make a statement about the thermal front progression.

The pulse tests were controlled through a programmable controller. This provided excellent control over pulse durations and switching procedure. For the baseline test, first a quick test with 6 pulses of 2x10-minute was performed. After that, 7 pulses of 2x1-hour was performed. Finally, a test with 5 pulses of 2x2-hours was performed. In the post-loading test, we employed 6 pulses of 93 minutes higher and 147 minutes lower injection rates. These therefore constitute 4-hour pulses but with the uneven time distribution between higher and lower rates more Fourier components in the frequency spectrum were expected.

## 3. RESULTS

### 3.1. The Geothermal System

#### 3.1.1 Rates and Pressures, and Frequency Content

The injection rates and pressures imposed and measured in the new well, I2, are represented in Figure 1. We observe that the pressure drops below zero during the lower injection rates. This indicates that the fluid level has dropped below the location of the pressure gauge in that part of the test. As a consequence, poor quality are expected.

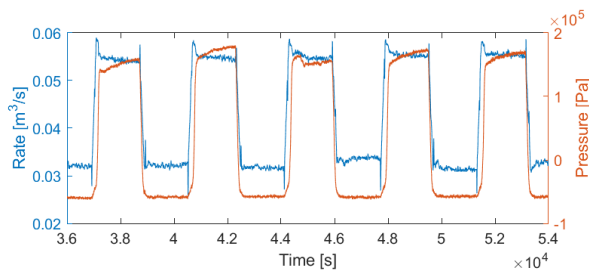


**Figure 1** Imposed rates and measured pressures of the pulse test in the geothermal well I2. The lower-than-zero, virtually constant pressures during the lower injection rates indicate the fluid level being below the pressure gauge

Higher pressures were experienced in well I1, in line with the expectations from earlier injection tests that indicated smaller injectivity. The employed rates and the measured pressures are represented in Figure 2.

From the test in injector I1 we identified the frequency components present in the responses. The results in terms of frequency spectra of the rate and the pressure are given in Figure 3. The response is calculated after identifying the frequencies associated with the applied pulses – these are given by the peaks in the frequency spectrum and should correspond with  $f_i = \frac{i}{T}$ , with  $i = 1, 3, \dots$ . We can identify some 15 frequency peaks.

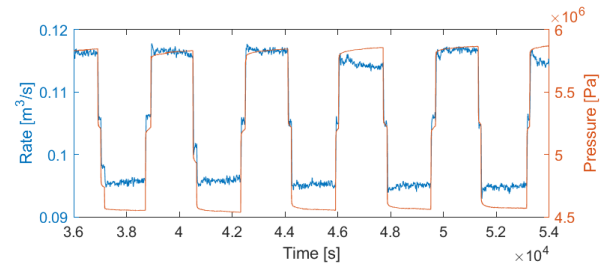


**Figure 2** Imposed rates and measured pressures of the pulse test in the geothermal well I1.

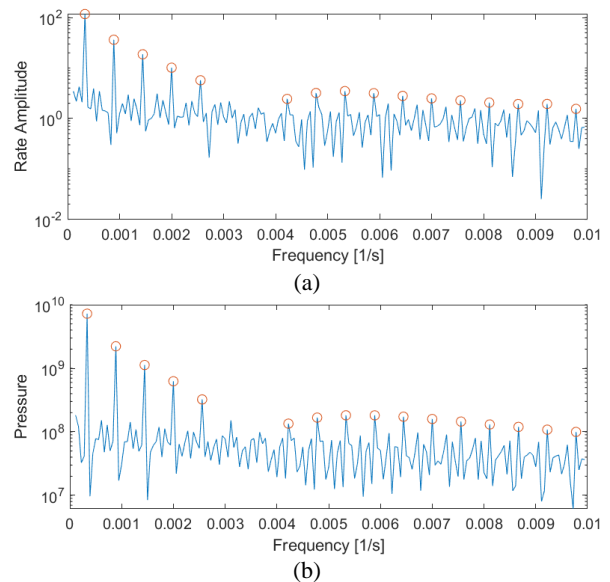


**Figure 3** Frequency spectra of the imposed rates (a) and the measured pressures (b) of the pulse test in the geothermal well I1. The 6<sup>th</sup> and 7<sup>th</sup> theoretical pulses have been excluded since their amplitude does not exceed the background enough.

#### 3.1.2 Analysis

The response is calculated by comparing the pressure frequency information by the rate frequency information for the frequencies identified. This gives two direct pieces of information: the ratio of the amplitudes and the phase delay between the two signals. In addition, we calculated the amplitude response derivative in the period domain. This procedure has been explained in Fokker et al (2021). It was designed to help the pulse test analysis and facilitate a pressure-derivative analysis method resembling what is common in regular well testing practice. We focus here on the pressure and the pressure derivative signals.

Only a few harmonic components were available for the analysis of the geothermal system (Figure 3). For both wells,

interpretation was characterized by a high degree of uncertainty because the horizontal stabilizations on pressure derivative, corresponding to water at reservoir temperature and water at injection temperature, were not observable. This is due, on one side, to the wellbore storage hump covering the near wellbore stabilization and, on the other side, to an investigated area of the aquifer not far enough to reach the transition zone. For well I1 the attempt of interpretation is shown in Figure 4a. We estimated a horizontal permeability of 800 mD ( $h=26$  m) and an apparent skin of 12 ( $C=2e-7$  m<sup>3</sup>/Pa), reflecting both the effect of injecting a cooler fluid, characterized by a lower mobility, and the presence of an already developed cooler zone around the well. In fact, in well I1 the test has been performed after two years of injection, resulting in an expected thermal front around 600 m.

For well I2 the attempt of interpretation shown in Figure 4b, provided a horizontal permeability of 1500 mD ( $h=39$  m) and an apparent skin of 1 ( $C=8e-6$  m<sup>3</sup>/Pa), reflecting mainly the effect of injecting a cooler fluid. In this case the lower apparent skin may be interpreted as a not yet developed cooler zone around the well. These results are in line with the injection history of the two wells. The high wellbore storage value obtained for both interpretation, mainly due to the presence of gas in the water, is in line with the interpretation results of build-up tests already available.

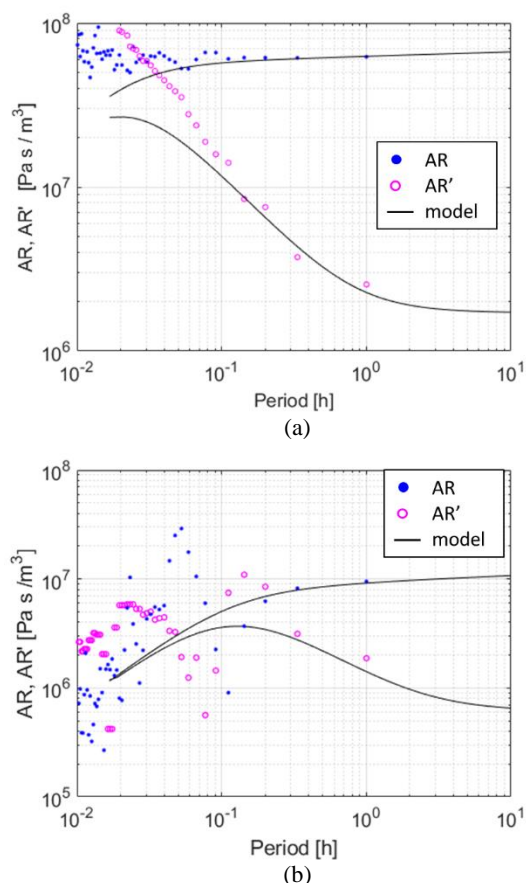


**Figure 4** Interpretation of the amplitude ratio (AR) and amplitude ratio derivative (AR') response of (a) well I1 and (b) well I2, respectively.

### 3.2. The Heat Store System

#### 3.2.1 Rates and Pressures, and Frequency Content

The baseline investigation comprised three pulse tests, with 6 pulses of 2x10-minute duration, 7 pulses of 2x1-hour and a

test with 5 pulses of 2x2-hours. The rates and pressures versus time are represented in Figure 5.

After heat loading, one test with 6 pulses of 93 minutes higher and 147 minutes lower injection rates was performed. With the uneven time distribution between higher and lower rates more Fourier components in the frequency spectrum were expected. The imposed rates and resulting pressures are represented in Figure 6.

A peculiar and unexpected feature of the pressure development for the pulses after the loading is that some time after the moment of switching the growth (for increased rate) and decline (for decreased rate) change into decline and growth, respectively. We found that this may be due to temperature variations, which appeared to also have happened during this test. A representation of the temperature at the position of the pump at 135 m depth, and the calculated temperature at the depth of the perforations, is provided in Figure 7. We leave the incorporation of the temperature for later analysis.

As in the Geothermal System, we here also identified the frequency components present in the responses. Especially the tests with longer pulse durations give many useable peaks in the frequency spectrum; Figures 8 and 9 give the responses of the 4-h baseline test and the post-loading test, respectively.

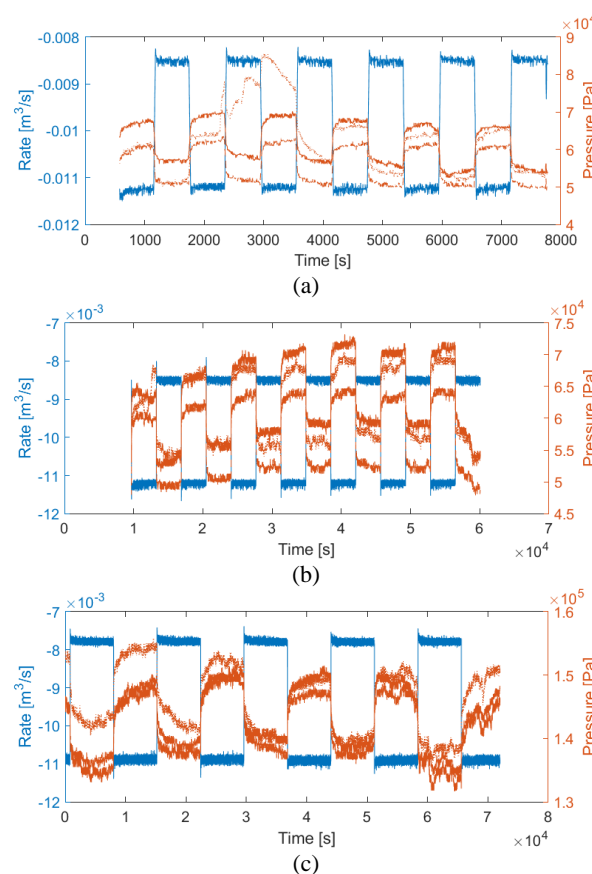


**Figure 5** Injection rates and resulting pressures for the baseline pulse tests in the heat storage system: (a) six pulses of 2x10 min, (b) 7 pulses of 2x1-hour and (c) 5 pulses of 2x2-hours. For each test, pressure traces P1 and P3 are compared.

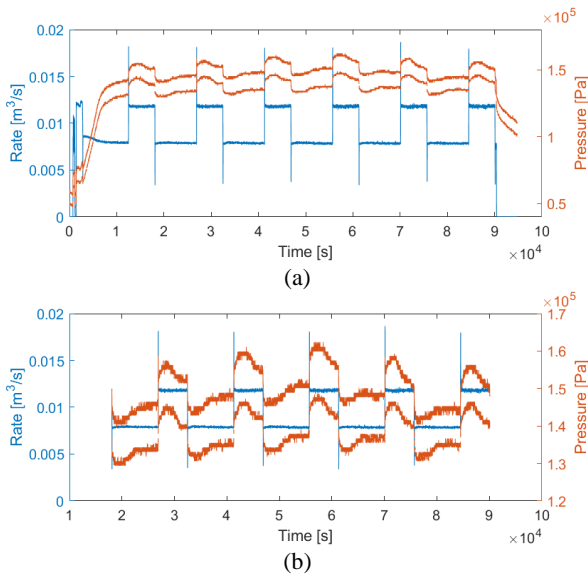


**Figure 6 Rates and pressures for the post-loading test in the heat storage system: (a) entire test and (b) subsection extracted for the interpretation.**

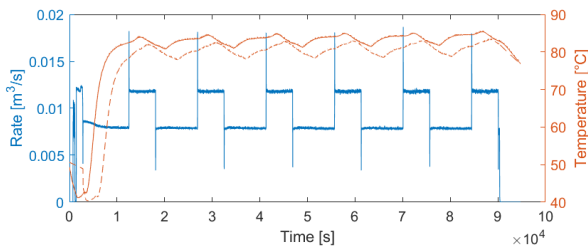


**Figure 7 Rates and temperatures for the post-loading test in the heat storage system. Solid line: temperature at the pump location. Dashed line: calculated bottomhole temperature**

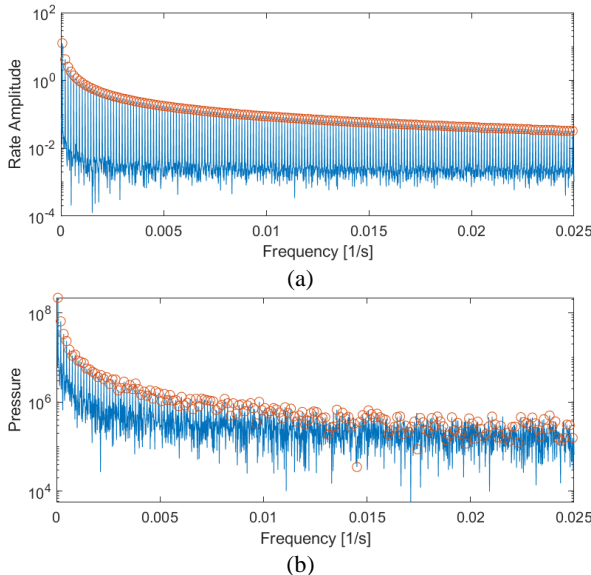


**Figure 8 Frequency spectra of the imposed rates (top) and one of the measured pressures traces (bottom) of the 5x4-hour baseline pulse test in the heat storage well.**

(a)

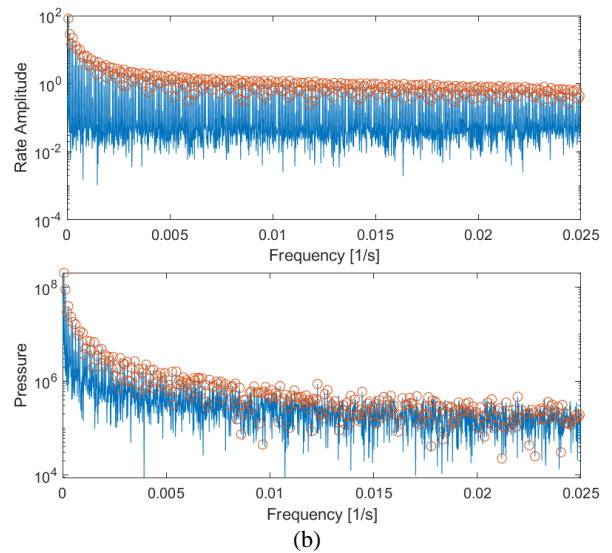


**Figure 9 Frequency spectra of the imposed rates (a) and the measured pressures (b) of the 5x4-hour post-loading pulse test in the heat storage well.**

### 3.2.2 Analysis

Results from the three baseline tests are compared in Figure 10. The three derivatives show very similar behaviour, characterized by an initial horizontal stabilization, a transition zone and a second horizontal stabilization. However, the 20 minutes period test is too short to identify the second stabilization. Even if the data and corresponding derivative are affected by noise, the horizontal stabilization corresponding to injected fluid mobility and reservoir mobility are detectable and in good agreement on both baseline tests and post-loading test (Figure 10 – 11 and Figure 12, respectively). It is pointed out that in the baseline tests, when a heated area around the well has not yet developed and the thermal front advances significantly during the test, the horizontal stabilization corresponding to reservoir mobility is detectable on the left side of the plot (corresponding to low periods and high frequencies), before the one corresponding to injected fluid mobility (Figure 10 – 11) This behaviour is similar to what was observed with the interpretation of injection periods in injection tests in oil and gas fields (Levitan, 2002; Verga et al., 2011; Verga et al., 2014). Post loading test shows a conventional behaviour with the reservoir stabilization following the near wellbore one, since a significant warmed area is already present around the wellbore.

The interpretation of the pressure derivative of post-loading test has been performed as outlined in Fokker et al (2021). The pressure derivative as obtained from the measurements have been used to determine the driving parameters by fitting the output of the theoretical response to the field response. The result, of which the match is shown in Figure 13, provided a horizontal permeability of 3000 mD, an thermal interface radius (corresponding to the equivalent thermal front radius) of 100 m and a mobility ratio of 3.14, in agreement with the viscosity contrast between water at 15.5 °C (reservoir temperature) and at 85.5°C (injection temperature).

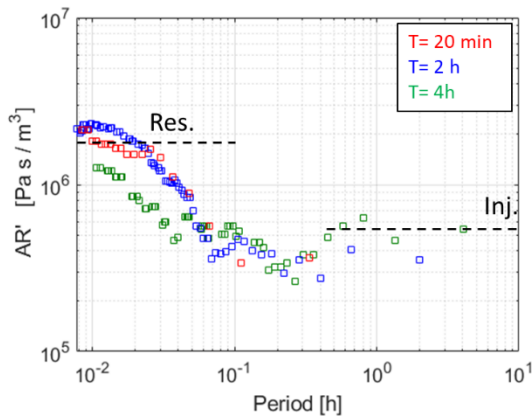


**Figure 10** Derivative responses of the three baseline pulse tests (gauge 3) in heat storage system and identification of horizontal stabilization to reservoir temperature mobility (Res.) and injection temperature mobility (Inj.)

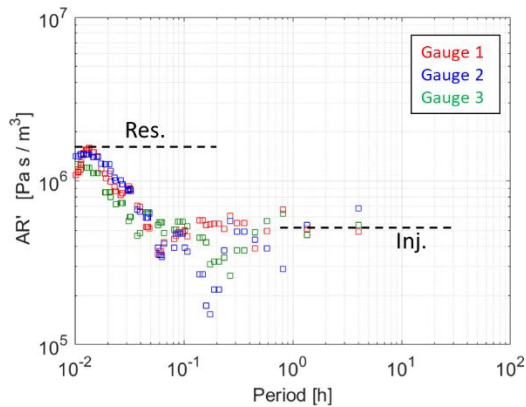


**Figure 11** Derivative responses of the baseline pulse test T=4h in heat storage system and identification of horizontal stabilization to reservoir temperature mobility (Res.) and injection temperature mobility (Inj.); comparison among the three gauges response.

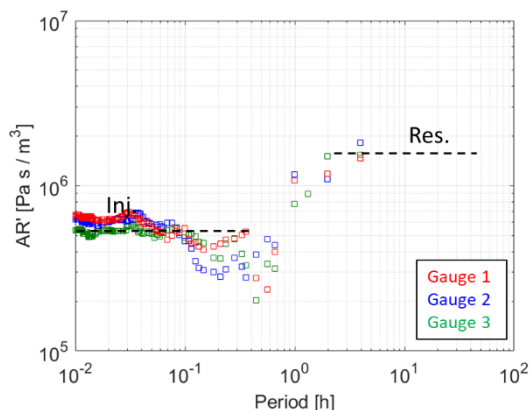


**Figure 12** Derivative responses of the post-loading pulse test in heat storage system and identification of horizontal stabilization to reservoir temperature mobility (Res.) and injection temperature mobility (Inj.); comparison among the three gauges response.

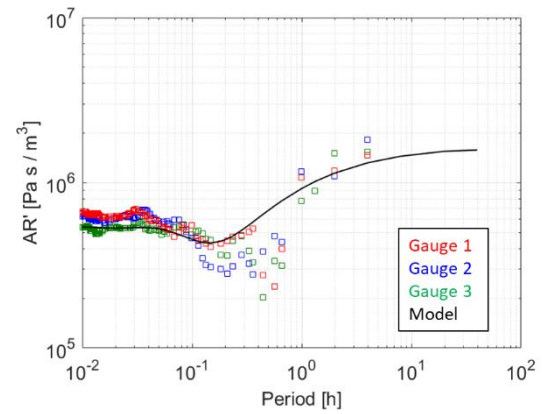


**Figure 13** Interpretation of the derivative responses of the post-loading pulse tests in heat storage system.

#### 4. DISCUSSION

For the geothermal system, the test was not completely successful. In fact, only a qualitative indication of the presence of a cooled front was obtainable from the interpretation. For a quantitative estimation, longer tests would be needed. For instance, a test with oscillation period of at least one week should be employed for well I1. Furthermore, an induced pressure difference higher than few bars would be desirable for a robust test interpretation.

Conversely, interpretation of the tests for the heat storage system provided a consistent quantitative estimation of the warmed area. The estimated thermal front radius (100 m) is in agreement with the one than can be calculated analytically for thermal convection only (about 101 m), assuming injected water at an average rate of 40 m<sup>3</sup>/h for 236 days and piston-like displacement. Thermal dissipation between water and rock should reduce the estimated thermal front radius by a factor (Benson and Bodvarsson, 1986):

$$\sqrt{\frac{\rho_w c_{vw}}{\rho_r c_{vr}}} \phi \approx 0.78$$

where  $\rho_w$  is the density of the water;  $\rho_r$  is the density of the rock;  $c_{vw}$  and  $c_{vr}$  are the specific heat of water and rock respectively;  $\phi$  is the porosity.

The thermal exchange between water and rock (conduction) acts over a significantly longer time-scale than thermal convection. The 8-months timespan of the loading operations should show thermal conduction limited to few meters, much less than the convective transport 100 m into the reservoir.

The amplitudes of the pressure response in the heat storage case were larger than predicted with the matched model. This may be related to the varying temperature, or with near-wellbore issues leading to negative skin values. This is subject of current research.

The heat storage case is part of a large investigation into the potential of high-temperature storage of heat in aquifers. Other studies are performed on other aspects of this system. One of those is the monitoring of the temperature in a nearby monitoring well. Another investigation concerns the use of different geophysical techniques like electric monitoring of the injection operations. Some first results of the other studies are reported separately (Dinkelman et al, 2022).

## 5. CONCLUSIONS

We have observed that indeed it is possible to establish the temperature and the size of the cooled or heated zone around the injector. The identification is established by comparing the frequency content of the imposed rate with the corresponding frequency content of the resulting pressure. However, the quality of the monitoring results depends on a number of physical and operational constraints.

The approximation made in the evaluation is about the geometry of the cooled or heated zone: it is assumed to be radially symmetric, homogeneous, and with a well-defined thermal radius. While these conditions are not met in practice, they are reasonable if the distortion from radial symmetry is not too severe and if a baseline is taken before injection has started. The monitoring then can focus on the differences with the original situation.

The operational conditions during a pulse test need to be defined carefully, on a case by case basis. A first issue here is the duration of the pulses. They must be long enough to be able to discriminate the thermal radius. At the same time, they must be defined precisely enough in order to maximize the short-time, near-well responses. Further, their amplitude must be large enough for a sizeable signal to develop at as many as possible frequencies. And finally, the pressure measurements should be taken as close to the reservoir as possible to minimize uncertainty and noise originating from the viscous and possibly turbulent flow in the well. Prior to the test, sensitivity calculations are necessary to quantify the requirements.

The tests performed were not ideal for the geothermal system, which limited the conclusive power of our interpretation. For the heat storage system, however, we have been able to make definite conclusions about the reservoir system properties and their changes after a period of injection. The heated area was in line with the volumetric consideration based on the amount of injected hot water. Also, the tests have helped to formulate operational constraints and factors for improvement. Pulse testing has the potential of becoming an important, and relatively cost-effective monitoring tool for water injector wells.

## REFERENCES

- Benson, S.M., Bodvarsson, G.S., Nonisothermal effects during injection and falloff tests. *SPEREE 1* (1), 53–63 SPE 11137-PA. (1986).
- Dinkelman, D., Carpentier, S., Koenen, M., Oerlemans, P., Godschalk, B., Peters, E., Bos, W., Vrijlandt, M and van Wees, J.D. High temperature aquifer thermal energy storage performance in Middenmeer, the Netherlands: thermal monitoring and model validation. EGC, Berlin, 2022.
- Fokker, P. A., Borello, E. S., Viberti, D., Verga, F., and van Wees, J. D.: Pulse Testing for Monitoring the Thermal Front in Aquifer Thermal Energy Storage. *Geothermics*, 89, (2021), 101942.
- Levitan, M.M., Application of Water Injection/Falloff Tests for Reservoir Appraisal: New Analytical Solution Method for Two-Phase Variable Rate Problems. Paper SPE 77532-MS presented at the SPE Annual Technical Conference and Exhibition, San Antonio, Texas, 29 September-2 October (2002).
- Verga F., Viberti D., Salina Borello E. and Serazio C. An Effective Criterion to Prevent Injection Test Numerical Simulation from Spurious Oscillations. *Oil Gas Sci.*

Technol. – Rev. IFP Energies nouvelles. Volume 69, Number 4, pp. 633 – 651. Dossier: Geosciences Numerical Methods. (2014)

Verga F., Viberti D., Salina Borello E., A new insight for reliable interpretation and design of injection tests, *Journal of Petroleum Science and Engineering*, Volume 78, Issue 1, , Pages 166-177, (2011) ISSN 0920-4105, <https://doi.org/10.1016/j.petrol.2011.05.002>.